Scanning Microscopy

Volume 7 | Number 3 Article 5

8-14-1993

Nanometer-Scale Synthesis and Atomic-Scale Modification with the Scanning Tunneling Microscope

Reginald M. Penner
University of California Irvine

Follow this and additional works at: https://digitalcommons.usu.edu/microscopy

 Part of the Biology Commons

Recommended Citation

Penner, Reginald M. (1993) "Nanometer-Scale Synthesis and Atomic-Scale Modification with the Scanning Tunneling Microscope," *Scanning Microscopy*: Vol. 7 : No. 3 , Article 5.
Available at: https://digitalcommons.usu.edu/microscopy/vol7/iss3/5

This Article is brought to you for free and open access by the Western Dairy Center at DigitalCommons@USU. It has been accepted for inclusion in Scanning Microscopy by an authorized administrator of DigitalCommons@USU. For more information, please contact digitalcommons@usu.edu.

Scanning Microscopy, Vol. 7, No. 3, 1993 (Pages 805-813)
Scanning Microscopy International, Chicago (AMF O'Hare), IL 60666 USA

0891-7035/93$5.00+.00

NANOMETER-SCALE SYNTHESIS AND ATOMIC-SCALE MODIFICATION WITH THE SCANNING TUNNELING MICROSCOPE

Reginald M. Penner

Institute For Surface and Interface Science (ISIS), Department of Chemistry
University of California Irvine, Irvine, CA 92717-2025

Telephone number: 714 856 8572 / FAX number: 714 856 8571

(Received for publication June 14, 1993, and in revised form August 14, 1993)

Abstract

The structure or composition of a surface may be locally altered in either of two fundamental ways using the scanning tunneling microscope (STM). A modification of the surface may be induced resulting in the rearrangement and/or removal of surface atoms, or in the transfer of atoms from the tip to the sample surface. In many recent experiments, the modification of surfaces has involved a single atom or an ensemble of a few atoms. Alternatively, the localized synthesis of a new material from reactants external to the STM tip and sample can be induced using at least three experimental strategies. A typical distance scale involved in such experiments is 10 nm (i.e., the smallest lateral dimension of the material synthesized). Progress in the areas of localized modification and localized syntheses with the STM (with greater emphasis on the latter) is summarized in this review.

Key Words: Scanning tunneling microscope (STM), atomic force microscope (AFM), field evaporation, chemically assisted field evaporation (CAFE), metal dichalcogenides, electrochemical, lithography, modification, deposition, synthesis, patterning, nano-structure.

Introduction

In addition to providing the means for viewing surfaces a very high magnification in a non-perturbative fashion, the scanning tunneling microscope (STM) can be employed to locally change the structure or composition of a surface. This change may involve either the *modification* of the surface structure, or the localized *synthesis* of a new compound on the surface. The distinction between surface modification and synthesis is a useful one for this review and a more explicit definition of these terms is attempted next.

Modification will be narrowly defined to mean the removal of atoms from the surface, the reorganization of surface atoms, or the transfer of atoms from the STM tip to the surface. By this definition, the first STM modification experiment was reported by Becker *et al.* [6], who in 1987 described the manipulation of atoms on germanium surfaces. In recent publications (*vide infra*), the scale of the modification has been atomic: involving either a single atom or an ensemble of a few atoms. A further advance has been the induction and observation of dynamic phenomena at surfaces. For experiments at gold [23, 36, 37] and silicon surfaces [34, 35], for example, rapid modification (or restructuring) of the surface results in a displacement from the equilibrium structure which is followed by relaxation to a new equilibrium structure. These experiments provide evidence of rapid progress in the area of surface modification and several excellent reviews of this area have recently appeared [3-5, 57]. A further review of this area will not, therefore, be undertaken here. Instead, the **Modification** section will focus on surface modification experiments involving surfaces of the layered metal dichalcogenides (e.g. MoS_2, $SnSe_2$, etc.) for which unique and somewhat controversial data have been recently obtained.

The **synthesis** of a new material from precursor species involves a chemical reaction induced in the STM. As compared with surface modification experiments, several distinct differences can be identified:

a). *Precursor species external to the surface and tip are necessarily involved.* Precursor molecules (or

atoms) may be located on the surface (e.g., in a thin, solid film), in a contacting gas phase, or in a contacting solution phase. Surface atoms can participate as precursors, of course, as in the reaction of the silicon atoms of a Si(111) surface with gaseous O_2 to form SiO_x.

b). *Surface synthesis occurs on a* ***minimum*** *distance scale of* $\approx$ *1 nm.* Provided the product of a synthesis reaction in the STM is a crystalline material (e.g., the compound semiconductor cadmium selenide), the nano-phase produced by synthesis will not possess the mechanical and electronic properties characteristic of the material on a distance scale smaller than the smallest unit cell dimension (e.g., $\approx$ 5.4-6.5 Å for semiconductors [27]). So far, this theoretical limit has not been approached and it has proven difficult to prepare materials having a smallest dimension of less than $\approx$ 10 nm.

c). *The exact nature of the modification is less apparent.* In view of the relative distance scales involved, this fact is surprising. However, the surface structure associated with an atomic scale modification can be (and has been [c.f. 34, 35]) unambiguous from STM images of the modified region alone. This can virtually never be said for a nanometer-scale synthesis experiment: The elemental composition, the crystal structure (or crystallinity), and the homogeneity of a protrusion formed by a nanometer-scale chemical process in the STM is not revealed in STM images of the nanostructure, and the minuscule quantities of material involved often thwarts characterization by conventional surface analytic methods. The characterization problem is an unavoidable consequence of the chemical complexity of the materials for which a synthesis is attempted, and the fact that the highest standards of surface cleanliness cannot be maintained (as in ultra high vacuum, UHV) due to the presence of the precursor species in the system.

Atomic Scale Modification of Surfaces

The physics by which individual atoms may be picked up, translated, and deposited on surfaces by manipulations of the bias, current, and tip position in the STM was incompletely understood in early experiments. However, a growing data library [c.f. 1, 2, 6, 17, 19-21, 23, 25, 34-37, 57] has guided the development of theoretical models [4, 5, 29, 45, 46, 55, 56] which provide physical and chemical insight to the mechanism of atomic scale modification phenomena. A useful theoretical description of atom transfer, which is specific to the STM, is the chemically assisted field evaporation (CAFE) model advanced by Avouris and coworkers [c.f., 4, 5] and elaborated by Lang [30]. CAFE successfully explains the experimental observations pertaining to a diverse range of atomic scale modification phenomena including the transfer of physisorbed xenon atoms between a tungsten tip and at Ni(110) surface at 4°K [19, 20], the deposition of small gold clusters on a Au(111) surface from a gold tip at room temperature [36, 37], and the atomic scale manipulation of silicon atoms on Si(111) surfaces at room temperature [23]. As already noted, these data have been recently reviewed [3-5]. In the paragraphs below, experiments involving the atomic scale modification of layered, two-dimensional (2-D) materials is examined in light of the CAFE description.

The layered metal dichalcogenides (examples of which include MoS_2, $SnSe_2$, and WSe_2) are van der Waals crystals in which covalently bonded, triatomic thick layers (e.g., S-Mo-S) are stacked to form a three dimensional material having extremely anisotropic electronic properties. Whereas the van-der Waals surfaces of these crystals can be extremely chemically inert, the atomic scale modification of these surfaces using the STM and the atomic force microscope (AFM) has been the subject of a number of recent publications [1, 2, 14, 21, 25, 49]. Single atoms, or clusters of a few atoms, can be extracted from defect-free regions of the surfaces of MoS_2 and $SnSe_2$ in UHV [25], and from WSe_2 surfaces in air [21] by the application of bias pulses in the STM. Lieber *et al.* [25] have attributed the extraction of atoms to an electric field effect based on the observation of material dependent bias pulse thresholds for the removal of atoms from the surface: For MoS_2 and $SnSe_2$ surfaces in UHV, the observed bias pulse thresholds of -3.5 $\pm$ 0.3 V and -1.4 $\pm$ 0.2 V (tip negative), respectively, correlate with the known metal-chalcogenide bond strength which is greater for MoS_2 [25]. Figure 1 shows STM images of MoS_2 (left) and $SnSe_2$ (right) surfaces following the bias pulse-induced removal of atoms in the STM. Once formed, the vacancies created at the surface are quite stable either in air [c.f. 14, 21] or in UHV [25] when the surface is not subjected to imaging with the STM (or AFM).

Chalcogenide vacancies, which are either induced with the STM or which are present as defects in the material [14], serve to nucleate the two dimensional, layer-by-layer etching of layered material during STM imaging. This effect has been observed for $NbSe_2$, TaS_2, $MoSe_2$, $TiSe_2$ [49], WSe_2 [1, 49], MoS_2, and $SnSe_2$ [25, 49]. With continued STM imaging of a missing atom site, particularly at large tip-sample bias [1, 25, 49], an etch "crater", one layer in depth, grows from the missing atom site. With some materials (e.g., WSe_2 [1], $NbSe_2$ [49]), etch craters have a triangular shape and an orientation which is dictated by the symmetry of the layer which is being removed [49]. Delawaski and Parkinson [14] have shown that etching reactions indistinguishable from those which are observed with the STM are induced by imaging with the AFM. An example is the sequence of AFM images of a $SnSe_2$ surface shown in Figure 2 in which the complete removal of a single Se-Sn-Se trilayer and the partial removal of a second such layer can be seen to occur at an applied force of 80 $\pm$ 20 nN [14]. By changing the force applied to the surface in the AFM, the effect of the physical tip-surface interaction on the etching rate can be assessed in the absence of an applied electric field. In experiments of this type conducted by Delawaski and Parkinson [14], an etching rate which was directly proportional to the applied force was observed suggesting

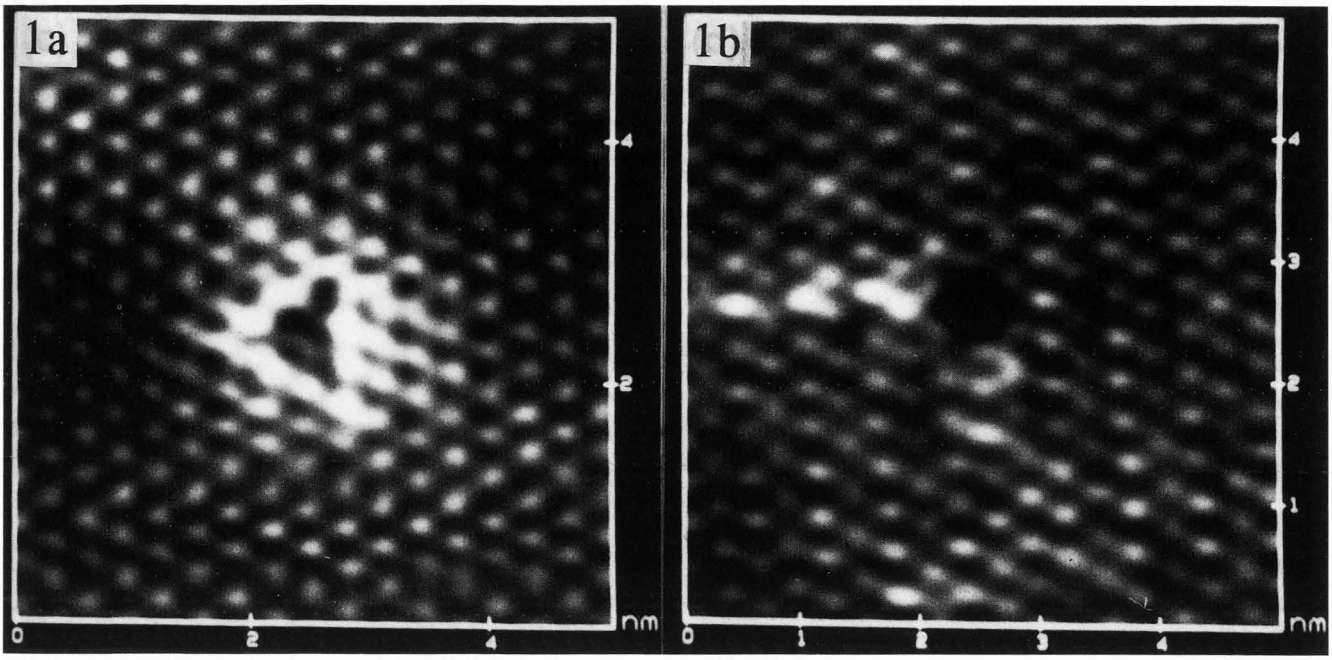

Figure 1 (above). Atomic resolution STM images of the surfaces of $SnSe_2$ (**a**) and MoS_2 (**b**) following the extraction of a single atom. These modifications were brought about by the application of tip-positive bias pulses of 1.4 V and 3.5 V, respectively, in UHV. From reference 26. Reprinted with permission, Copyright 1992, American Institute of Physics.

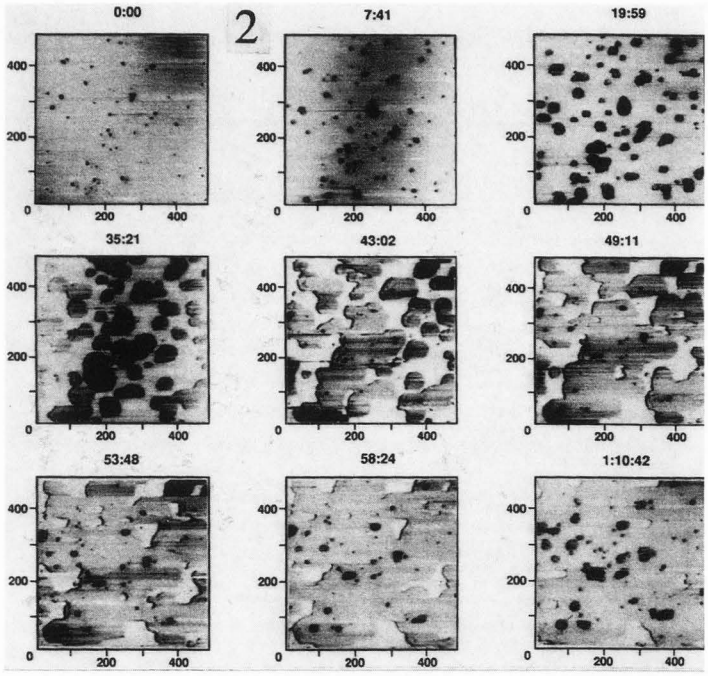

Figure 2 (at right). AFM images of a single 500 x 500 nm region of a $SnSe_2$ surface during repetitive imaging at an applied force of 80 $\pm$ 20 nN in air. From reference 14. Reprinted with permission, Copyright 1992, American Chemical Society.

that the physical interaction of the STM tip with the surface (instead of the electric field or the current) is primarily responsible for etching in the STM. In contrast, in the STM experiments conducted by Lieber *et al.* [25], bias amplitude thresholds of -1.7 V and -4.5 V for $SnSe_2$ and MoS_2 were observed for the onset of 2-D etching in UHV. This observation supports a field-assisted desorption mechanism for atom extraction, similar to the mechanism responsible for the transfer of metal between an STM tip and a surface [36, 37].

Qualitatively, these apparently disparate conclusions can both be reconciled with the CAFE description of atom transfer [4, 5, 30]: The time, τ, required for an atom to thermalize over the potential energy barrier, Q, separating adsorption at the surface and at the tip is given by the equation of Müller [47]:

$$\tau = \tau_o e^{(Q/kT)} \qquad (1)$$

where τ_o is the vibrational time constant for vibration

along the reaction coordinate, perpendicular to the surface. With the approach of the STM (or AFM) tip to a surface, a lowering of Q occurs as the potential energy surface for atoms at the surface merges with the potential energy surface for atoms adsorbed at the tip [4, 5, 30]. The magnitude of this "proximity" or "chemical" effect is large at small tip-sample separations: Lang [30] has calculated a rate of barrier height lowering equal to $\approx$ 1 eV/Å for the transfer of a silicon atom between two jellium-model electrodes. A dramatic increase in the atom transfer rate, $1/\tau$, is therefore predicted (by Eq. 1) to accompany a decrease in the tip-sample distance either in the STM or in the AFM, as increased force is applied as in the experiments of Delawaski and Parkinson [14]. Extrapolation of the results of Lang [30] for the jellium/silicon system reveals that $Q \approx kT$ should be attained at a tip-sample distance of $\approx$ 3.5 Å at 300°K. At this separation, which may be inaccessible with an STM under normal imaging conditions, transfer of the silicon atom should occur in the absence of an applied electric field with a frequency approximately equal to $1/e\tau_o$.

Directionality is imparted to the atom transfer as a consequence of the dissimilar chemical forces acting at a tip and at a surface having different chemical compositions, and/or, in STM experiments, by the application of a bias pulse which induces ionization at the surface and the migration of charged species [4, 5, 30]. Since in the AFM experiments of Delawaski and Parkinson [14] atom transfer is observed in the absence of an applied field, the directionality of transfer (i.e., to the tip from the surface) is presumably due solely to a strong attractive interaction between atoms of the surface and the silicon nitride tip. For the larger tip-surface separations which probably exist in the STM experiments of Lieber *et al.* [25], a larger barrier to atom transfer likely exists which is surmounted only with the assistance of a field-assisted desorption mechanism of transfer at some elevated bias pulse amplitude. In summary, the AFM etching experiment of Delawaski and Parkinson [14] may represent an unusual case of CAFE operating at the high chemical interaction limit, whereas the STM etching observations of Lieber *et al.* [25] represents an intermediate chemical interaction case very similar to that encountered in the silicon atom extraction experiments of Lyo and Avouris [34, 35].

Nanometer-Scale Materials Syntheses on Surfaces

Nanometer-scale synthesis in the STM involves the reaction of precursor species, induced by current flow between the STM tip and the surface, to form a product which is deposited in a highly localized fashion on the surface. The disposition of the precursor species in the system forms the basis of a useful system of classification for the various synthetic strategies which have been demonstrated to date. The three possibilities are:

a) *Precursor molecules are disposed in a thin, solid film* on the substrate surface. A well known example are thin films of metal fluoride salts (e.g., CaF_2), a high resolution, positive tone, e-beam resist compound. Metal fluoride e-beam resists including MgF_2, AlF_3, LiF, and CaF_2 are "self developing" in the sense that a high dose of electrons (e.g., 1 C/cm^2) electron beam directly induces decomposition of the salt (e.g., MX_2) by the following reaction [7]:

$$MX_2 \text{ ---> } M^\circ + X_2 \qquad (2)$$

No separate development step, such as the dissolution step normally required for the development of polymer resists, is necessary. McCord and Pease [40] demonstrated for the first time in 1986 that the exposure of CaF_2 resists can be accomplished with 20 nm resolution using electrons from an STM tip during field emission operation of the instrument.

b) *(Volatile) precursor species are present in a contacting gas phase.* In an early example [53], cadmium was deposited using a scheme adapted from molecular organic chemical vapor deposition (MOCVD) methods: Volatile dimethyl cadmium, $Cd(CH_3)_2$, gas molecules accept or donate electrons in or near the tunneling gap in an STM to form a molecular anion which migrates to the substrate surface. Further reaction of this species is induced to occur, sometimes at elevated substrate temperatures, culminating in the deposition of elemental cadmium [7]:

$$Cd(CH_3)_2 + e^- \text{ ---> } Cd(CH_3)_{2^-(gas)}$$
$$\text{ ---> } Cd(CH_3)_{2^-(surface)} \qquad (3)$$

$$Cd(CH_3)_{2^-(surface)} \text{ ---> } Cd^\circ + 2\ CH_2CH_2 + H_2 \qquad (4)$$

c) *(Soluble) precursor molecules are dissolved in a contacting solution phase.* One of the first examples involved the localized photochemical etching of the surface of gallium arsenide by Lin *et al.* [33]. In this experiment, the etching reaction, involving water as a reactant, produces soluble products and the localized **removal** of material from the surface. Schneir *et al.* [52] demonstrated the first electrochemical **deposition** experiment involving the localized plating of gold from an aqueous solution onto a gold substrate surface:

$$AuCl_3 + 3e^- \text{ ---> } Au^\circ + 3Cl^- \qquad (5)$$

For syntheses experiments of this type, the deposited product (e.g., Au°) must be insoluble in the liquid phase in order that precipitation of the material at the substrate surface occurs.

Recent progress in the area of nanometer-scale synthesis is reviewed for each of these three categories in the paragraphs below.

Reactions of solid films

A logical extension of the STM lithography experiments with CaF_2 resists [40] is to other e-beam resist materials. McCord and Pease [42] have shown that exposure of poly-(methyl methacrylate) or PMMA resists in the positive tone mode is accomplished at tip-sample voltages as small as 20 V in the STM. The resolution attainable for PMMA at low voltage with the STM ($\approx$ 100 Å [42]), however, has been matched with high energy electron beams [8]. Similar resolutions have not been

attainable thus far for negative tone resists in high energy e-beams [7, 39]. Negative tone resists consist either of thin monomer films, in which case e-beam exposure initializes polymerization, or thin polymer films, where large electron doses induce cross-linking of polymer chains and the generation of a low solubility region [7]. During irradiation, resist which is external to the e-beam cross-section can be exposed by electrons which are elastically scattered from the substrate surface [15, 16, 38,39]. This phenomena limits the accessible resolution.

By using electrons from an STM tip to effect exposure, a significant improvement in the resolution has been demonstrated for a negative tone resist (Shipley Co., SAL-601-ER7), originally by Dobisz and Marrian [15, 16]. SAL-601 is a polymer type resist which undergoes cross-linking reactions in an electron beam. In recent experiments [38, 39], lines as narrow as 23 nm have been written on resists of SAL-601, 50 nm in thickness, on silicon using an STM operating in field emission mode at a tip-negative bias of 15 V [38]. Exposure occurs when the tip is moved at a constant lateral speed across the resist at these high biases, and imaging of the modified region is accomplished using a scanning electron microscope (SEM). Importantly, SAL-601 exposed using low voltage electrons from the STM is capable of functioning as a mask during reactive ion etching (RIE) of the surface [38]. Figure 3 shows a pattern obtained by exposure of a 50 nm thick SAL-601 resist film on GaAs with electrons from an STM tip at -25 V. Following exposure, the pattern was transferred to the surface by removal of 100 nm of the GaAs surface about the exposed region by RIE with BCl_3. RIE is an essential operation in the micro- or nanolithographic preparation of integrated circuitry.

The resolution attainable with the STM is superior to that which can achieved using a conventional high voltage e-beam source due to the much smaller cross-section of low energy electrons for scattering from the substrate surface [38, 39]. For example, a 10 nm diameter 50 kV electron beam yields line widths of 95 nm [38, 39] for resist films of SAL-601 which are 50 nm in thickness. In addition, STM exposed patterns exhibit greatly reduced proximity effects (also resulting from surface scattering) and superior "process latitude" (or the ability to expose lines having a range of widths by changing the energy of the incident electrons) [38, 39]. The primarily limitation of STM is the write speed which is much slower than for high energy electron beams. Nevertheless, based on the advantages demonstrated for STM-based e-beam lithography to date, the emergence of commercial STM-based lithography seems feasible [39].

Reactions of gas phase precursor molecules

Oxidation of the sample surface is a common example of a synthesis reaction involving the reaction of the gas phase precursor O_2 with atoms on the surface. For hydrogen-passivated Si(111) surfaces in air, for example, Dagata *et al.* [9, 10] have shown that the surface oxidation reaction is initiated (or accelerated) by STM imaging at tip-negative biases greater than 1.7 V. In STM images of a patterned surface, such as that shown in Figure 4 [10], lines which are imaged at this bias are recessed by $\approx$ 20 Å into the surface and possess widths of 35 nm. Time-of-flight secondary ion mass spectroscopy (TOF-SIMS) images of patterned regions confirm the localized incorporation of oxygen [9, 10]. A similar phenomena is observed for passivated surfaces [11] of the technologically important III-V materials including GaAs, $Al_xGa_{1-x}AsJ$ and $In_yGa_{1-y}As$ [12]. For these surfaces, passivation is achieved by exposure of the freshly etched surface to a dilute aqueous $P_2S_5/(NH_4)_2S$ solution [11-13]. Surface oxide is generated locally by imaging with large tip-negative biases of $\approx$ 4 V and a lateral resolution of $\approx$ 50 nm has been demonstrated [11].

Localized syntheses in the STM, in which surface atoms are not direct participants in the chemical reaction, have been demonstrated using precursors culled from chemical vapor deposition (CVD) procedures [7]. Conventional CVD reactions (which are, in general, poorly characterized) are induced by elevated substrate temperatures. For some metal organic precursor species, these reactions have been initiated by electron transfer from an STM tip operating in field emission mode within 20 Å of the surface [43, 44, 53]. If the tip is negatively biased, one possible scenario is that the molecular anion produced by reduction of the metal complex migrates to the sample surface in closest proximity to the STM tip prior to reacting and generating the product of interest. A variation on this experiment is to employ a laser, focused in the region of the tip on the surface, to selectively react and/or ionize precursor molecules [58, 59].

CVD-like precursors have been employed by McCord *et al.* [43] to prepare nanoscopic deposits containing tungsten from tungsten hexacarbonyl and by McCord and Awschalom [44] to deposit arrays of magnetic nano-dots (diameter = 10-30 nm) from the precursor iron pentacarbonyl. Deposition in both of these experiments occurs with the STM operating at large tip-negative biases of -15 V (W) or -27 V (Fe). The magnetic susceptibility of the deposited material, in the case of iron deposition, is indicated by measurements of nanostructures deposited inside the confines of a planar dc SQUID [44]. Elemental analysis of nanostructures prepared from volatile metal complexes reveals a significant carbon content [43, 44, 53]. The carbon impurity may derive either from decomposition of the organic ligands or from the presence of a surface contamination layer on the substrate.

Reactions of liquid phase precursor molecules

At surfaces which are immersed in polar solvents, the tip-sample bias applied in an STM can be adjusted to drive electrochemical reactions at both the tip and the sample. At the sample surface, material may be removed by anodic dissolution or corrosion reactions in which electrosynthesis yields soluble products. For silicon [48], gallium arsenide [33, 48], and silver selenide [54] surfaces, for example, etching reactions directed

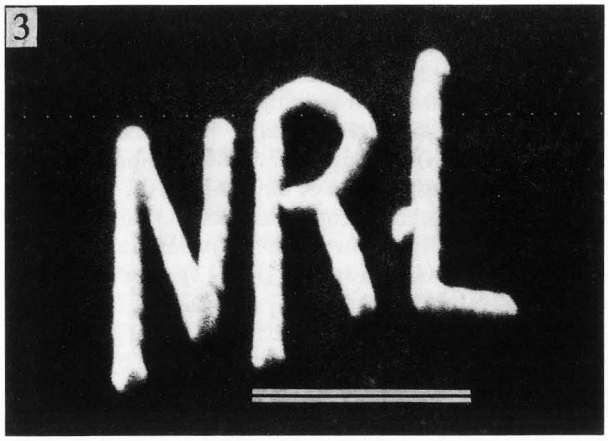

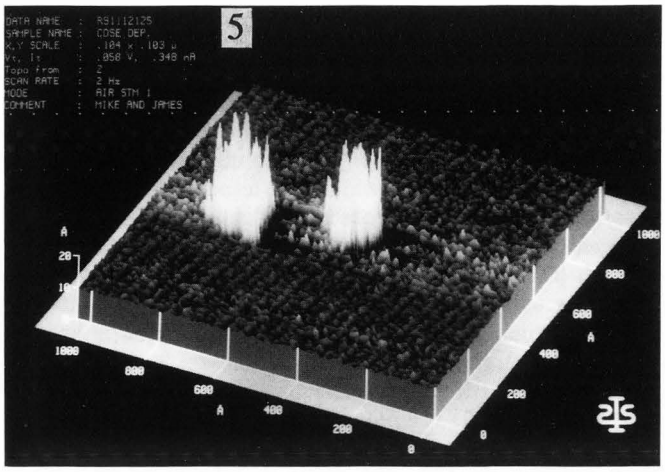

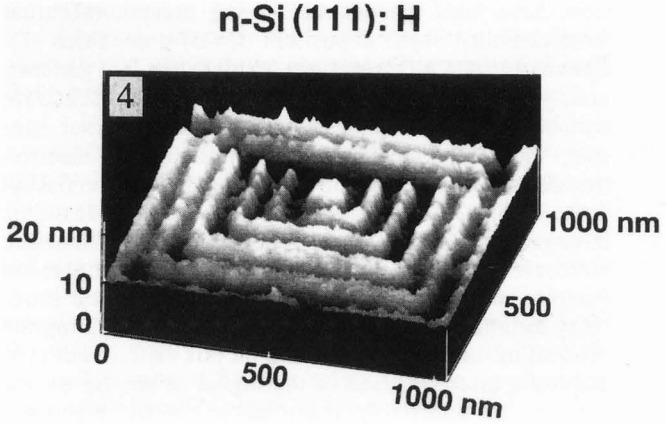

Figure 4. STM image of a pattern generated on a hydrogen terminated n-Si(111) surface with an STM operating in air. Lines were written with a tip-sample bias of 3.0 V and a tunneling current set-point of 3.0 nA; the STM image shown was then obtained using a tip-sample bias of 1.7 V and a current of 3.0 nA. From reference 10. Reprinted with permission, Copyright 1991, American Institute of Physics.

---

with the STM tip enable the formation of lines 10-20 nm in width which are recessed by 3-5 nm into the surface. In principle, and sometimes in practice, electrosynthesis reactions can be made to occur which generate an insoluble product such as a metal (e.g., for silver: $Ag^+ + 1e^-$ ---> Ag°, [26, 31]), a semiconductor (e.g., CdSe: *vide supra* [Li, Barsky, Virtanen and Penner, to be submitted]), an electronically conductive polymer (e.g., polythiophene), or an insulating and insoluble oxide (e.g., SiO_2). Due to the accessibility of many different types of electronic materials, nanometer-scale electrochemical synthesis in the STM has tremendous potential both technologically (since devices composed of a variety of electrosynthesized materials might be assembled) and for fundamental investigations of the chemistry and physics of nanometer scale materials.

Figure 3. Non-contiguous pattern obtained on a GaAs surface by exposure of a 50 nm thick SAL-601 resist using electrons from an STM tip operated at a tip-sample voltage of -25 V. Following exposure, the pattern was transferred onto the GaAs surface by reactive ion etching of the surface with BCl_3. From reference 37. Reprinted with permission, Copyright 1992, American Institute of Physics. Bar = 500 nm.

Figure 5. STM images of two nano-disk structures which were synthesized under conditions which favor the formation of cadmium selenide. Electrochemical synthesis was accomplished in an aqueous solution containing 1.0 m$\underline{M}$ $CdSO_4$, 0.3 m$\underline{M}$ SeO_3^{2-} using two +6 V x 50 μsec bias pulses. The STM image shown was obtained *in-situ* in the synthesis solution at a tip-sample imaging bias of $\approx$ +50 mV and a tunneling current of $\approx$ 0.2 nA using a polymer-insulated platinum STM tip.

On substrate surfaces having a low defect density, a pervasive problem with electrochemical deposition or synthesis, either of which involves the formation of a new phase, is that of nucleation. If it is assumed that metal deposition occurs by the so called "direct deposition model" [22], the importance of defect sites can be understood by analogy to the thermodynamic calculations of the redox properties of colloidal metal particles by Henglein [24]. In the general case, the reversible reduction of a metal cation, M^{n+} on a cluster composed of x atoms, can be written:

$$M^{n+} + M_x^\circ + ne^- \text{---} > M_{(x+1)}^\circ \quad E_{Mn+/M(x+1)^\circ} \qquad (6)$$

where $E_{Mn+/M(x+1)^\circ}$ is a standard electrode potential which is specific to the reduction of a single metal ion at a cluster of x metal atoms. For most metals, a positive shift of $E_{Mn+/M(x+1)^\circ}$ is predicted to occur as the number of atoms in the cluster increases from x = 1 [24]. In the case of silver, for example, the standard electrode

potential for formation of the first atom, $E_{Ag+/Ag1°}$, is -1.8 V versus normal hydrogen electrode (NHE). For reduction at a cluster of five silver atoms, $E_{Ag+/Ag6°} \approx +0.3$ V and for reduction at a large cluster or at a silver electrode surface, the macroscopic standard electrode potential, $E_{Ag+/Ago} = +0.799$ V, is realized [24]. Thus, a thermodynamic "nucleation overpotential" of 0.799 - (-1.8 V) ≈ 2.6 V can be calculated for the *homogeneous* reduction of silver in aqueous solution.

An analogous heterogeneous nucleation overpotential exists for deposition of silver onto the surface of any other metal. However, a favorable interaction of silver adatoms with atoms of the surface will result in a standard electrode potential for deposition of the first silver atom which is less negative than that predicted by Henglein [24]. The extent to which the surface reduces the total "surface" free energy of the first adatom depends on the local structure of the surface at the site of deposition: A less negative potential should suffice to initiate deposition at missing atom sites (≈ 5 coordinate) as compared with kink sites (≈ 3 coordinate) or step edges (≈ 2 coordinate). That is, deposition is thermodynamically favored at defect sites on the surface having the highest coordination number. The least thermodynamically favorable sites for deposition are atomically smooth regions of a crystalline substrate surface where interactions with atoms of the surface are minimized. **Importantly, the thermodynamic disparity between defect sites derives only from the phenomenon of nucleation and therefore, this disparity disappears following the deposition of the first few atoms.**

Thus, for electrochemical syntheses experiments, a picture emerges of the surface as consisting of an ensemble of defect sites each of which behaves as an ultramicroelectrode which is capable of initiating the synthesis reaction at a different potential. For this reason, it is not generally possible to confine an electrochemical synthesis reaction in the STM to an arbitrary site on a surface. In the worst case, if a defect-free region of a surface is selected as the incipient synthesis cite, the potential required for deposition there (including the large nucleation overpotential) will be more than sufficient to initiate the same synthesis reaction (but at much higher rates!) at a collection of nearby defect sites.

In principle, the problem of nucleation control is circumvented by employing some non-electrochemical mechanism to generate defects just prior to performing the electrochemical synthesis of interest. Mechanical modification of the surface with the tip is one possible method by which suitable defects might be produced (c.f., [41]). Another technique involves the formation of shallow pits by the application of large (> 4 V [50, 51]) amplitude bias pulses (of either polarity) between the STM tip and the basal plane surface of graphite, as originally demonstrated by Albrecht *et al.* [2]. Because pit formation occurs rapidly (< 5 μsec) as compared with electrochemical reaction rates, a single bias pulse having a duration of 50 μsec can be employed to generate a nucleation site on a graphite surface and to perform an electrochemical synthesis reaction, such as silver deposition. This integrated two-step mechanism of nucleation and electrochemical deposition has been successfully employed by Li *et al.* [31] to deposit silver nano-disks having diameters of ≈ 20-30 nm and heights of 2-7 nm. In these experiments, it was possible to locate silver nano-disks with a precision of a few nanometers on regions of a graphite surface which were initially defect free. Surprisingly, even when preexisting defects, such as step edges are nearby (i.e., within 50 nm), the silver reduction electrochemistry is completely confined to the pit formed in the graphite surface [31].

Using electrochemical synthesis, nanostructures of several materials may be synthesized in a single region of a graphite surface. Experimentally, this is accomplished by synthesizing one material using a solution containing the appropriate soluble precursors, exchanging this solution for a second solution containing the precursor species necessary for preparation of the second material, and performing the second electrosynthesis. Using this strategy, Li *et al.* [32] have deposited copper and silver nano-disk structures in close proximity to one another on a graphite surface, and subsequently monitored the reaction of these structures in a dilute Cu^{2+}-containing electrolyte. Discharge of this nanometer-scale galvanic cell occurs by the simultaneous dissolution of copper from the copper electrodes, and the deposition of approximately 2 monolayers of copper onto the silver electrodes via an under-potential deposition (UPD) mechanism [32] which was here-to-fore unknown (c.f., [29]). In this experiment, the STM functions as an ammeter capable of "measuring" currents as small as 10^{-18} A (corresponding to the transfer of 2 monolayers between copper and silver nano-structures over the course of 45 minutes, as observed) [32].

Electrochemical synthetic procedures for many of the group II-VI and group III-V semiconductors are known and these procedures are, in principle, adaptable to the nanometer scale electrochemical synthesis of semiconductor nanostructures in the STM. The feasibility of nanometer-scale semiconductor syntheses is demonstrated by the preparation of nanostructures under synthesis conditions favoring the formation of semiconducting n-type cadmium selenide [[Li, Barsky, Virtanen and Penner, to be submitted]. In this case, the synthesis reaction is a six electron reduction [28]:

$$Cd^{2+} + SeO_3^{2-} + 6H^+ + 6e^- \text{---} > CdSe + 3H_2O \quad (7)$$

Figure 5 shows two nanostructures - 200 Å in diameter and 20 Å in height which were synthesized from an aqueous solution containing 1.0 m$\underline{M}$ Cd^{2+} and 0.3 m$\underline{M}$ SeO_3^{2-}. Unlike metal nanostructures, CdSe nano-disks may be synthesized in very close proximity to one another (within 150 Å, in Figure 5, for example) on a graphite surface. Elemental analysis of these nanostructures, in order to ascertain the Cd:Se stoichiometry, is precluded by the minute quantity of material, and the fact that CdSe is a particularly electron beam sensitive material. However, a number of indirect indicators rule

out the possibility that the deposited material is either elemental selenium or cadmium metal [[Li, Barsky, Virtanen and Penner, to be submitted].

Acknowledgments

The author is grateful to Ph. Avouris, J. Dagata, R. Garcia, C. Lieber, S. Lindsay, H. Mamin, C. Marrian, M. McCord, and B. Parkinson for supplying reprints of papers, original line drawings, and STM images. Preprints of manuscripts prior to publication were generously supplied by Ph. Avouris, C. Marrian, and H. Mamin. Finally, the author thanks the Office of Naval Research, the National Science Foundation, the Arnold and Mabel Beckman Foundation, the Procter & Gamble Company, and the Petroleum Research Fund administered by the American Chemical Society, for the on-going financial support of research in the area of STM investigations of liquid-covered surfaces.

References

1. Akari S, Möller R, Dransfeld K (1991) Triangular structures on tungsten diselenide induced and observed by scanning tunneling microscopy. Appl. Phys. Lett. **59**: 243-245.

2. Albrecht TR, Dovek MM, Kirk MD, Lang CA, Quate CF, Smith DPE (1989) Nanometer-scale hole formation on graphite using a scanning tunneling microscope. Appl. Phys. Lett. **55**: 1727-1730.

3. Avouris Ph (1993) Atomic scale modification of materials. APS News. **2**: 90-92.

4. Avouris Ph, Lyo I-W (1992) Probing the chemistry and manipulating surfaces at the atomic scale with the STM. Appl. Surf. Sci. **60/61**: 426-436.

5. Avouris Ph, Lyo I-W, Hasegawa Y (1993) STM-induced modification and electrical properties of surfaces on the atomic and nanometer scales. In: Atomic and Nanometer-Scale Modification of Materials: Fundamental and Applications. Avouris Ph. (ed.). Kluwer Academic Publishers, Dordrecht, Netherlands. In press.

6. Becker RS, Golovchenko JA, Swartzentruber BS (1987) Atomic-scale surface modifications using a tunneling microscope. Nature **325**: 419-421.

7. Brodie I, Muray JJ (1992) The Physics of Micro/Nano Fabrication. Plenum Press, New York. pp. 1-150.

8. Craighead HG, Howard RE, Jackel LD, Mankiewich PM (1983) 10 nm linewidth electron beam lithography on GaAs. Appl. Phys. Lett. **42**: 38-40.

9. Dagata JA, Schneir J, Harary HH, Evans CJ, Postek MT, Bennett J (1990) Modification of hydrogen-passivated silicon by a scanning tunneling microscope operating in air. Appl. Phys. Lett. **56**: 2001-2003.

10. Dagata JA, Schneir J, Harary HH, Bennett J, Tseng W (1991) Pattern generation on semiconductor surfaces by a scanning tunneling microscope operating in air. J. Vac. Sci. Technol. **B9**: 1384-1388.

11. Dagata JA, Tseng W Bennett J, Schneir J, Harary HH (1991) Passivation of GaAs surfaces for scanning tunneling microscopy in air. Appl. Phys. Lett. **59**: 3288-3290.

12. Dagata JA, Tseng W, Bennett J, Schneir J, Harary HH (1991) Nanolithography on III-V semiconductor surfaces using a scanning tunneling microscope operating in air. J. Appl. Phys. **70**: 3661-3665.

13. Dagata JA, Tseng W (1993) Ambient scanning tunneling spectroscopy of n- and p-type gallium arsenide. Appl. Phys. Lett. **62**: 591-593.

14. Delawaski E, Parkinson BA (1992) Layer-by-layer etching of two dimensional metal chalcogenides with the atomic force microscope. J. Am. Chem. Soc. **114**: 1661-1667.

15. Dobisz EA, Marrian CRK (1991) Sub-30 nm lithography in a negative electron beam resist with a vacuum scanning tunneling microscope. Appl. Phys. Lett. **58**: 2526-2528.

16. Dobisz EA, Marrian CRK (1991) Scanning tunneling microscope lithography: a solution to electron scattering. J. Vac. Sci. Technol. **B9**: 3024-3027.

17. Dujardin G, Walkup RE, Avouris Ph (1992) Dissociation of individual molecules with electrons from the tip of a scanning tunneling microscope. Science **255**: 1232-1235.

18. Ehrichs EE, Yoon S, de Lozanne AL (1988) Direct writing of 10 nm features with the scanning tunneling microscope. Appl. Phys. Lett. **53**: 2287-2289.

19. Eigler DM, Lutz PC, Rudge WE (1991) An atomic switch realized with the scanning tunneling microscope. Nature **352**: 600-603.

20. Eigler DM, Schweizer EI (1991) Positioning single atoms with a scanning tunneling microscope. Nature **344**: 524-526.

21. Garcia RG (1992) Atomic-scale manipulation in air with the scanning tunneling microscope. Appl. Phys. Lett. **60**:1960-1962.

22. Harrison JA, Thirsk HR (1971) The fundamentals of metal deposition. In: Electroanalytical Chemistry, Vol. 5. Bard AJ (ed.). Marcel Dekker, New York. pp. 67-148.

23. Hasegawa Y, Avouris Ph (1992) Manipulation of the reconstruction of the Au(111) surface with the STM. Science **258**: 1763-1765.

24. Henglein A (1993) Physiochemical properties of small metal particles in solution: "Microelectrode" reactions, chemisorption, composite metal particles, and the atom-to-metal transition. J. Phys. Chem. **97**: 5457-5471.

25. Huang J-L, Sung Y-E, Lieber CM (1992) Field-induced surface modification on the atomic scale by scanning tunneling microscopy. Appl. Phys. Lett. **61**: 1528-1530.

26. Hüsser OE, Craston DH, Bard AJ (1988) High-resolution deposition and etching of metals with a scanning tunneling microscope. J. Vac. Sci. Technol. **B6**: 1873-1876.

27. Kittel CK (1986) Introduction To Solid State Physics. Sixth Edition. Wiley/Interscience, New York. Chapter 1, pp. 3-25.

28. Kressein AM, Doan W, Klein JD, Sailor MJ

(1991) Synthesis of stoichiometric cadmium selenide films via sequential monolayer electrodeposition. Chem. Mat. **3**: 1015-1018.

29. Laguren-Davidson L, Lu F, Saleita GN, Hubbard AT (1988) Electrodeposition of Bi, Pb, Tl, and Cu at Ag(111) from aqueous solutions. Studies by Auger spectroscopy and low-energy electron diffraction. Langmuir **4**: 224-232.

30. Lang ND (1992) Field induced transfer between two closely spaced electrodes. Phys. Rev. **B45**: 13599-13606.

31. Li W, Virtanen JA, Penner RM (1992) Nanometer-scale electrochemical deposition of silver on graphite using scanning tunneling microscopy. Appl. Phys. Lett. **60**: 1181-1183.

32. Li W, Virtanen JA, Penner RM (1992) A nanometer-scale galvanic cell. J. Phys. Chem. **96**: 6529-6531.

33. Lin CW, Fan F-R F, Bard AJ (1987) High resolution photochemical etching of n-GaAs with the scanning electrochemical and tunneling microscope. J. Electrochem. Soc. **134**: 1038-1039.

34. Lyo I-W, Avouris Ph (1990) Atomic scale desorption processes induced by the scanning tunneling microscope. J. Chem. Phys. **93**: 4479-4480.

35. Lyo I-W, Avouris Ph (1991) Field-induced nanometer- to atomic-scale manipulation of silicon surface with the STM. Science **253**: 173-176.

36. Mamin HJ, Chiang S, Birk PH, Guethner PH, Rugar D (1991) Gold deposition from a scanning tunneling microscope tip. J. Vac. Sci. Technol. **B2**: 1398-1402.

37. Mamin HJ, Guethner PH, Rugar D (1990) Atomic emission from a gold scanning tunneling-microscope-tip. Phys. Rev. Lett. **65**: 2418-2420.

38. Marrian CRK, Dobisz EA, Dagata JA (1992) Electron-beam lithography with the scanning tunneling microscope. J. Vac. Sci. Technol. **B10**: 2877-2881.

39. Marrian CRK, Dobisz EA, Dagata JA (1993) Low voltage e-beam lithography with the STM. In: The Technology of Proximal Probe Lithography. Marrian CRK (ed.). Proceedings SPIE, Bellingham, WA. In press.

40. McCord MA, Pease RFW (1986) Exposure of calcium fluoride resist with the scanning tunneling microscope. J. Vac. Sci. Technol. **B4**: 86-88.

41. McCord MA, Pease RFW (1987) The scanning tunneling microscope as a micromechanical tool. Appl. Phys. Lett. **50**: 569-571.

42. McCord MA, Pease RFW (1988) Lift-off metallization using poly-(methyl methacrylate) exposed with a scanning tunneling microscope. J. Vac. Sci. Technol. **B6**: 293-296.

43. McCord MA, Kern DP, Chang THP (1988) Direct deposition of 10-nm metallic features with the scanning tunneling microscope. J. Vac. Sci. Technol. **B6**: 1877-1880.

44. McCord MA, Awschalom DD (1990) Direct deposition of magnetic dots using a scanning tunneling microscope. Appl. Phys. Lett. **57**: 2153-2155.

45. Miskovsky NM, Wei CM, Tsong TT (1992) Field evaporation of gold in single- and double-electrode systems. Phys. Rev. Lett. **69**: 2427-2430.

46. Miskovsky NM, Tsong TT (1992) Field evaporation of silicon in the field ion microscope and scanning tunneling microscope configurations. Phys. Rev. **B46**: 2640-2643.

47. Müller EW (1956) Field desorption. Phys. Rev. **102**: 618-624.

48. Nagahara LA, Thundat T, Lindsay SM (1990) Nanolithography on semiconductor surfaces under an etching solution. Appl. Phys. Lett. **57**: 270-272.

49. Parkinson BA (1990) Layer-by-layer nanometer-scale etching of two dimensional substrates using the scanning tunneling microscope. J. Am. Chem. Soc. **112**: 7498-7502.

50. Penner RM, Heben MJ, Lewis NS, Quate CF (1991) Room temperature subnanometer scale lithography on liquid-covered graphite using scanning tunneling microscopy. Appl. Phys. Lett. **58**: 1389-1391.

51. Schimmel Th, Fuchs H, Akari S, Dransfeld K (1991) Nanometer-size surface modifications with preserved atomic order generated by voltage pulsing. Appl. Phys. Lett. **58**: 1039-1041.

52. Schneir J, Hansma PK, Elings V, Gurley J, Wickramasinghe K, Sonnenfeld R (1988) Creating and observing surface features with a scanning tunneling microscope. Proceedings SPIE **897**: 16-19.

53. Silver RM, Ehrichs EE, de Lozanne AL (1987) Direct writing of submicron metallic features with a scanning tunneling microscope. Appl. Phys. Lett. **51**: 247-249.

54. Utsugi Y (1990) Nanometre-scale chemical modification using a scanning tunneling microscope. Nature **347**: 747-749.

55. Walkup RE, Newns DM, Avouris Ph. The role of multiple inelastic transitions in atom-transfer with the STM. Phys. Rev. **B 48**: 1858-1861.

56. Walkup RE, Newns DM, Avouris Ph. (1993) Vibrational heating and atom transfer with the STM. In: Atomic and Nanometer-Scale Modification of Materials: Fundamental and Applications. Avouris Ph (ed.). Kluwer Academic Publishers: Dordrecht, Netherlands. In press.

57. Whitman LJ, Stroscio JA, Dragoset RA, Celotta RJ (1991) Manipulation of adsorbed atoms and creation of new structures on room-temperature surfaces with a scanning tunneling microscope. Science **251**: 1206-1210.

58. Yau S-T, Saltz D, Nayfeh MH (1991a) Laser-assisted deposition of nanometer structures using a scanning tunneling microscope. Appl. Phys. Lett. **57**: 2913-2915.

59. Yau S-T, Saltz D, Nayfeh MH (1991b) Scanning tunneling microscope - laser fabrication of nanostructures. J. Vac. Sci. Technol. **B2**: 1371-1375.

Editor's Note: All of the reviewers' concerns were appropriately addressed by text changes, hence there is no **Discussion with Reviewers**.